



Cite this: DOI: 10.1039/d5ma00694e

GeS mixed-dimensional 1D nanowire–2D plate heterostructures on van der Waals substrates

Eli Sutter ^{*ab} and Peter Sutter ^c

Vapor–liquid–solid (VLS) growth is widely used to synthesize 1D semiconductor nanostructures with high yield and crystal quality. Recently, the VLS concept has been extended from 3D-crystalline semiconductors to 2D/layered van der Waals crystals, *e.g.*, providing nanowires and mixed-dimensional heterostructures of the layered semiconductor GeS. However, Au-catalyzed growth of GeS nanostructures on silicon is invariably limited to small, sparse areas. Here, we report how this issue can be overcome *via* epitaxial VLS growth on van der Waals substrates, in the present case quasi-continuous SnSe films on mica. We show that Au-catalyzed VLS growth on SnSe yields complete coverage with mixed-dimensional GeS heterostructures combining 1D nanowires and 2D plates. Transmission electron microscopy and electron diffraction demonstrate that the nanowire backbone and the attached plates have the same crystal structure and layer orientation, with the [001] (van der Waals) direction aligned along the axis of the nanowire, templated by the basal plane of the underlying SnSe film. In contrast to GeS nanowires grown on Si, which invariably include screw dislocations and are thus chiral (with Eshelby twist), GeS nanowires formed on SnSe are layered single crystals that do not contain any dislocations. The optoelectronic properties of individual 1D–2D GeS heterostructures, probed by cathodoluminescence, draw on their unique architecture incorporating a sequence of GeS plates with intense luminescence and size-tunable emission wavelengths. Our results pave the way for the high-yield synthesis of a wide range of layered nanostructures using epitaxial VLS growth on van der Waals substrates.

Received 30th June 2025,
Accepted 5th November 2025

DOI: 10.1039/d5ma00694e

rsc.li/materials-advances

1. Introduction

There has been a lot of interest in creating heterostructures of 2D/layered crystals.¹ A distinct class of heterostructures combines components of different dimensionality, *e.g.*, 1D elements such as nanowires, nanorods, or nanotubes are integrated with 2D plates, sheets, or belts, into a hybrid architecture.² These hetero- or mixed-dimensional heterostructures are often of interest for applications that benefit from a large surface area. Mixed-dimensional heterostructures have been constructed from various conventional 3D-crystalline materials (*i.e.*, crystals with covalent bonding in all three dimensions), including oxides, noble metals, and semiconductors. For instance, CdS–ZnIn₂S₄ nanowire–nanoplate heterostructures have been found to facilitate charge transfer and enhance the performance of photoelectrochemical cells.³ FeS–Co₃O₄ nanowire–nanosheet heterojunctions showed improved

photoelectrochemical water splitting.⁴ CdSe–CdS nanorod–nanoplate heterostructures exhibited enhanced activity for photocatalytic hydrogen evolution compared to single-component CdSe nanorods and CdS/CdS homostructures,⁵ while Au–PdAg nanorod–nanosheets showed enhanced electrocatalytic hydrogen evolution.⁶

Recently, mixed-dimensional heterostructures integrating conventional 3D crystals with layered van der Waals crystals have been attempted as well. For example, CdS–Cu_{2–x}S/MoS₂ nanorod–nanosheet architectures with high photocatalytic activity have been successfully produced.⁷ CdS–WSe₂ ribbon-flake heterostructures served as waveguide-integrated LEDs in dual-role modules for optoelectronic circuitries.⁸ Combining graphene with SiC whiskers appears promising for boosting electricity generation,⁹ while ZnO nanowire–WSe₂ heterojunction diodes showed enhanced rectification.¹⁰

Judiciously combining van der Waals crystals in mixed-dimensional heterostructures may offer an easier path towards producing functional architectures. Following this strategy, layered Cu_{2–x}S nanowires were decorated by dense ensembles of small (sub-10 nm) MoS₂ and MoSe₂ nanosheets using edge epitaxy in solution.¹¹ Combining PbI₂ nanowires and WSe₂ sheets led to enhanced excitonic emission,¹² Bi₂S₃ nanowires combined with WS₂ monolayers improved the performance of

^a Department of Mechanical and Materials Engineering, University of Nebraska–Lincoln, Lincoln, NE 68588, USA. E-mail: esutter@unl.edu

^b Nebraska Center for Materials and Nanoscience, University of Nebraska–Lincoln, Lincoln, NE 68588, USA

^c Department of Electrical and Computer Engineering, University of Nebraska–Lincoln, Lincoln, NE 68588, USA



photodetectors,¹³ while GeS nanowires templated their twist into GeSe shells.¹⁴ Carbon nanotubes paired with MoS₂ sheets suggest a new solution for tunneling transistors owing to electron transfer between them.¹⁵ So far such heterostructures have mostly combined components of both different dimensionality and different materials, and were usually fabricated by sequential synthesis or transfer.^{3–7,11–13,15}

Combining the same van der Waals crystals in mixed-dimensional heterostructures requires that a particular material can be stabilized in both dimensionalities. In general, 1D–2D integration of the same material would be facilitated for layered materials that can be synthesized as 2D flakes as well as 1D nanowires, preferably with the same stacking orientation. This possibility has already been demonstrated for GeS, a semiconducting layered group IV monochalcogenide of interest for optoelectronics and twistrionics. GeS nanowires and plates can be spontaneously integrated during vapor–liquid solid (VLS) growth,¹⁶ as well as in a more complex two-step process.¹⁷ Using the same approach, the single-step synthesis of heterostructures combining GeS_{1–x}Se_x alloy nanowires and plates with different compositions has been achieved as well.¹⁸ Despite the successful demonstration of GeS based 1D–2D heterostructures, their VLS synthesis on Au-covered Si substrates so far has remained challenging, mainly due to frustrated nucleation that is typically limited to a few areas on the substrate. In addition, VLS growth generally yields a mixture of both 1D nanowires and 1D–2D mixed-dimensional heterostructures. A change of the catalyst from Au to Bi enhanced coverage to the entire surface but eliminated the formation of mixed-dimensional heterostructures, limiting the growth to GeS nanowires only.¹⁹ Recently, VLS growth of PbI₂ on PbI₂ thin films has demonstrated dense arrays of aligned nanowires.²⁰ Here we explore the possibility of overcoming the limited growth and achieving full coverage of the entire substrate by mixed-dimensional GeS heterostructures using van der Waals crystals as support. Specifically, we investigate the Au-catalyzed VLS growth of GeS on films of SnSe, group IV monochalcogenide that is isostructural with GeS. We use optical microscopy, scanning electron microscopy (SEM), atomic force microscopy (AFM) and transmission electron microscopy (TEM) and electron diffraction to demonstrate coverage of mixed-dimensional GeS heterostructures across the entire substrate, and to investigate their structure and morphology. We find that the formation of GeS heterostructures requires the presence of Au catalyst on the van der Waals support. Finally, we use cathodoluminescence spectroscopy to investigate the optoelectronic properties of the mixed-dimensional GeS heterostructures.

2. Results and discussion

GeS nanowires and mixed-dimensional heterostructures were grown on two types of substrates, Si(100) and SnSe/mica, in a quartz tube reactor with two independently controlled temperature zones using GeS vapor transport in Ar carrier gas (see Methods for details). Prior to the growth, thin Au films

(with equivalent thickness between 2–10 nm) were deposited by magnetron sputtering on Si(100) and SnSe/mica substrates. The Au films dewet at the growth temperature to generate a poly-disperse array of supported Au nanoparticles that serve as VLS catalysts.²¹

2.1. GeS nanowires and mixed-dimensional heterostructures grown on Au/Si

Exposure of the Au-catalyst to pure GeS vapor results in the formation of GeS nanostructures. On Si(100), the GeS growth invariably appears limited to a few areas on the substrate surface (Fig. 1(a)), despite the fact that the Au film uniformly covers the entire Si surface. The Au-catalyzed GeS growth on Si(100) results in formation of isolated patches of concentric rings of different structures, including forests of nanowires at the center (Fig. 1(a) and (b)). The surface of the Si substrate away from these growth areas is uniformly covered with an array of Au particles (Fig. 1(c) – left). At the periphery of the growth areas, the Au particles are larger than in the surrounding substrate regions and appear brighter in SEM, indicating uptake of GeS from the vapor phase (Fig. 1(c) – right). In the central region, finally, we invariably observe the formation of nanowires carrying 2D plates, *i.e.*, mixed-dimensional heterostructures (Fig. 1(d) and (e)), whose length reaches a maximum at the very center. GeS nanowires^{22,23} and nanowires decorated with plates^{16,17} have been successfully prepared earlier under similar conditions. SEM images of 90° tilted samples (Fig. 1(e)) show the individual standing mixed-dimensional GeS heterostructures that can accommodate 2D plates with different spacing and thickness. Importantly, both plan-view and tilted SEM images show that the GeS nanowires do not grow directly on the Au covered Si substrate but on thick GeS deposits.

The deposits appear to consist of GeS plates with different thicknesses preceding the growth of GeS nanowires and mixed-dimensional heterostructures and providing a substrate for their growth in the isolated concentric areas. The GeS plates are thicker at the center and gradually become thinner and inclined in different directions toward the periphery. SEM images show GeS nanowires and heterostructures growing vertically on these GeS plates. Our observations suggest that the presence of van der Waals crystals as support is a key requirement for the VLS growth of wires and mixed-dimensional heterostructures. However, on Au/Si substrates these GeS van der Waals plates are synthesized spontaneously only in very limited parts of the Si substrate (making it impossible to predict their position), and are inhomogeneous in thickness and orientation (hence carrying wires at random angles relative to the average substrate surface). The limiting factor determining the formation of GeS nanowires or mixed-dimensional heterostructures can therefore be identified as the spontaneous nucleation of GeS plates in small areas of the Si substrate, where they provide a van der Waals support for the subsequent epitaxial growth of VLS nanostructures.

SEM images show the presence of Au-rich catalyst particles with bright contrast on the surface of the GeS deposits and at nanowire tips. The presence of an Au-rich catalyst particle at



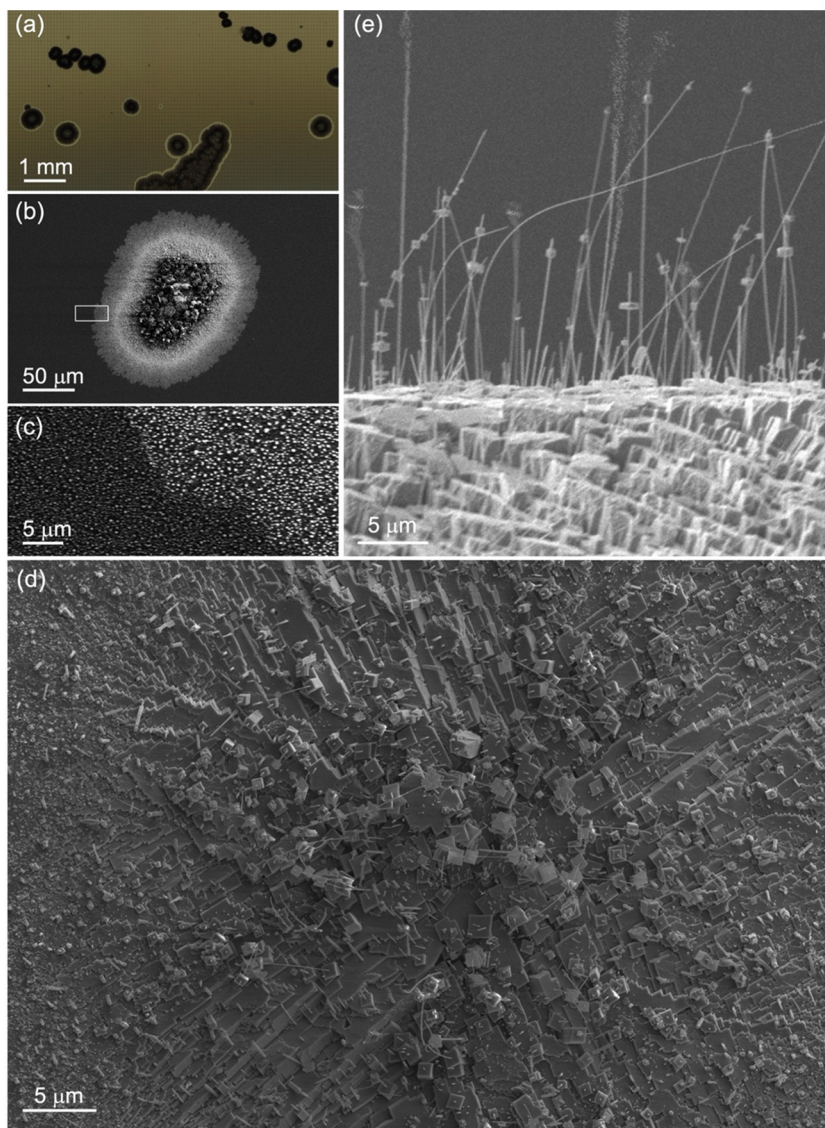


Fig. 1 GeS nanowire-plate heterostructures on the Au/Si(100) substrates. (a) Overview optical image of GeS growth on Au/Si(100). (b) Top-view SEM image of GeS nanowires with and without plates grown as isolated patches of concentric forests on Au/Si(100) substrates. (c) Higher magnification SEM image of the periphery of the growth area (rectangle in (b)), showing a transition between the layer of Au particles formed after the dewetting of the Au on Si(100) and the area where some uptake of GeS has occurred as demonstrated by the different contrast and increased size of the particles. (d) Top-view SEM image of the center of a concentric growth area. Growth of GeS nanowires with and without plates generally occurs only in areas that are covered with a thick GeS layer. Frequently short segments of nanowires carrying the growth catalyst emerge from the layer. (e) Side-view SEM images of GeS nanowires with and without plates, grown on the thick GeS layer on the growth substrate. The 1D-2D hybrids form by introduction of plates with different sizes at different positions along the GeS nanowires.

every tip of the mixed-dimensional heterostructures supports the earlier finding that the growth of the GeS nanowires proceeds *via* the vapor-liquid-solid mechanism^{22,24} while the formation of the plates can be explained by the direct incorporation of GeS molecules from the vapor phase at certain position along the nanowires. Such vapor-solid growth of the 2D plates attached to the sidewalls of nanowires has also been observed for mixed-dimensional heterostructures of GeS_{1-x}Se_x alloys, where it yields a different composition (*x*) of the plates compared to the VLS-grown wires.¹⁸

TEM investigation of the nanowires grown on Au/Si(100) confirms the presence and distribution of plates along their

length (Fig. 2(a)-(c)). Electron diffraction shows that morphologically, the GeS nanowires and plates are longitudinally stacked with the GeS *c*-axis parallel to the nanowire axis (Fig. 2(d)). Consistent with previous results, a large majority of the GeS nanowires grown on Au/Si substrates show the presence of a single axial screw dislocation. The dislocation induces characteristic Eshelby twist, which manifests itself in gradual and continuous changes in nanobeam electron diffraction patterns along the nanowires, a telltale sign of the progressive rotation of the in-plane (*a*, *b*) planes around the nanowire axis (Fig. 2(d)),^{19,25} independent of the presence of plates decorating the nanowires.



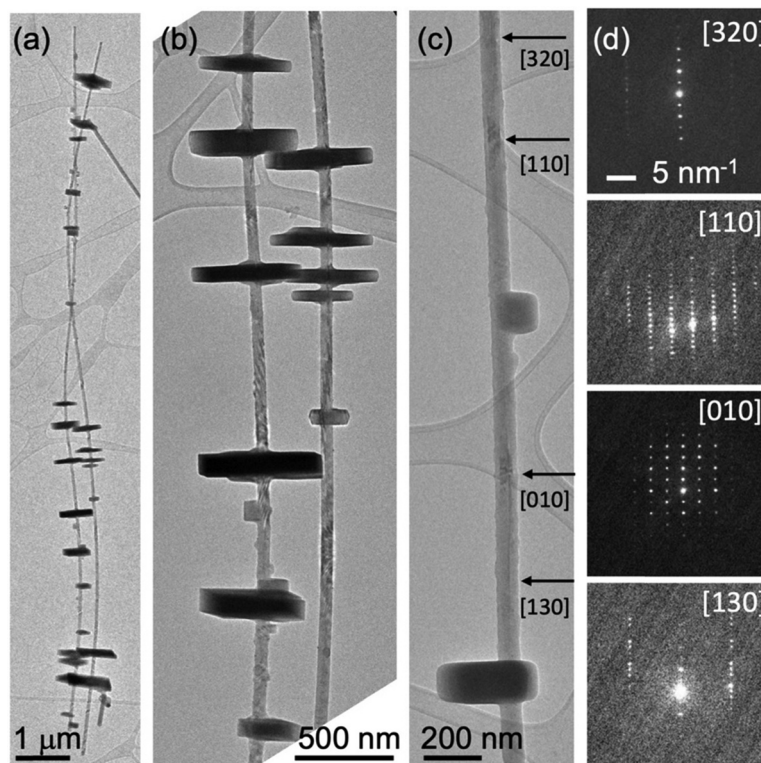


Fig. 2 Twist in Au-catalyzed GeS mixed-dimensional heterostructures synthesized on Si(100). (a)–(c) TEM images of characteristic GeS nanowires decorated with multiple plates at different positions grown over Au catalyst at a substrate temperature of 300 °C (dispersed on lacey carbon support). (c) Segment of a nanowire with small plates along which a sequence of 300 nanobeam electron diffraction patterns were measured. Arrows indicate the positions at which the nanowire is viewed along particular zone axes with indices $[h\ k\ l]$. (d) Selected nanobeam electron diffraction patterns at the positions marked by arrows in (c). The diffraction patterns denote the actual zone axis: $[320]$, $[110]$, $[010]$ and $[130]$, of the nanowire and show progressive twist of the (a, b) crystal axes along the nanowires between the plates.

2.2. GeS nanowires and mixed-dimensional heterostructures grown on Au/SnSe/mica

GeS growth was further carried out on Au-covered SnSe films on mica. Growth on SnSe without Au did not result in any nanowire growth. The SnSe films were prepared in a separate reactor – for details see the Materials and Methods section below. Combined imaging using optical microscopy, SEM, and AFM shows that SnSe deposition on mica substrates results in formation of quasi continuous layers composed of individual, partially overlapping SnSe flakes (Fig. 3). The size of the SnSe flakes typically ranges between 10–30 μm . The flakes coalesce, attach, and overgrow one another forming a continuous film. Polarized optical microscopy (Fig. 3(a)) shows repeated areas with the same contrast, indicating fused flakes with the same orientation and similar height. SEM (Fig. 3(b)) and AFM imaging (Fig. 3(c)) confirm the quasi-continuous nature of the van der Waals layers with flat basal-plane surfaces and typical height difference between consecutive levels in the range of 20–100 nm, correlated with the typical thickness of the intergrown flakes. The quasi-continuous SnSe film provides a large, flat van der Waals surface for the deposition of the 2 nm Au film and the subsequent GeS nanowires growth.

GeS growth on the Au/SnSe films on mica results in formation of dense forests of GeS nanostructures that cover the

entire substrate (Fig. 4(a)). This is a major difference to the growth on Si substrates where, as discussed above, GeS plates supporting GeS nanostructures form only in small, sparse circular areas of the support (Fig. 1). The forests consist of mixed-dimensional nanowire-plate heterostructures, as seen in higher magnification SEM images (Fig. 4(b)–(d)). EDS measurements in SEM confirm that the heterostructures consist of pure GeS (Fig. 4(e)).

TEM investigation demonstrates the presence and distribution of plates along the length of the nanowires grown on Au/SnSe films (Fig. 5(a)–(c) and Fig. S1(a)–(e)) and establishes their morphology. The TEM images show that the nanowires are decorated by plates attached at different positions along their lengths. The lengths of the heterostructures regularly extend over tens to hundreds of microns. High-resolution TEM images and electron diffraction (Fig. 5 and Fig. S1) establish that both the GeS nanowires and plates are longitudinally stacked with the GeS c -axis parallel to the nanowire axis.

Nanobeam electron diffraction confirms that both the nanowire segments and the attached plates consist of orthorhombic GeS;²⁶ SnSe from the support is not incorporated in the growing nanostructures. The nanowire sections consist of single crystalline GeS, whose layer structure seamlessly extends into the laterally attached GeS plates (Fig. 5(e)).



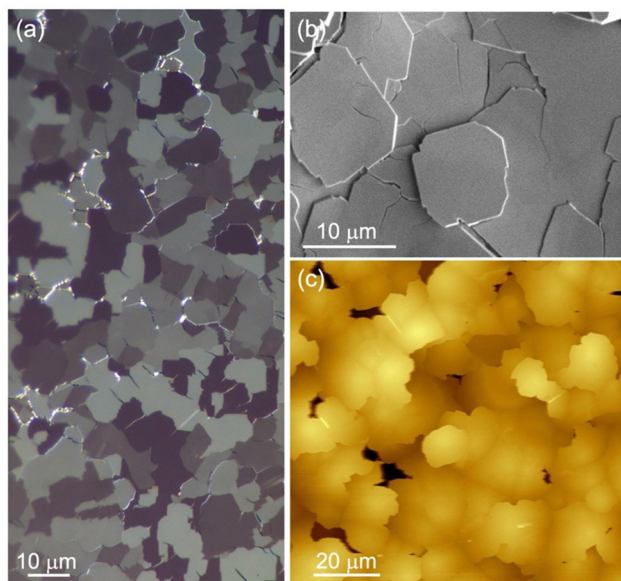


Fig. 3 Morphology of SnSe van der Waals support films grown on mica. (a) Polarized optical microscopy of a characteristic SnSe film on mica grown at 570 °C. (b) SEM and (c) AFM images of the SnSe films. Optical, SEM, and AFM imaging of the SnSe films shows that they consist of stacked individual plates with lateral sizes of 10–20 μm, whose top surfaces are terminated by the flat basal plane. The consecutive layers of the films form by merging of plates, frequently leaving isolated individual plates on the top surface.

Nanobeam electron diffraction (NBED) linescans (Fig. 6 and Fig. S1) show that the nanowires and heterostructures grown on

Au/SnSe/mica supports are single crystalline. However, while a large majority of GeS wires obtained on Au/Si carried axial screw dislocations and showed the transition between different zone axes characteristic of Eshelby twist (Fig. 2),^{19,25} GeS wires grown on Au/SnSe/mica show identical NBED patterns along their entire length (Fig. 6(b)), *i.e.*, these nanowires do not show any lattice rotation due to Eshelby twist but are viewed along the same crystallographic direction with fixed (*a*, *b*) crystal axes along the entire wires. Thus, in contrast to nanowires grown on Au/Si(100), the nanowires grown on the van der Waals support do not incorporate axial screw dislocations (and hence do not show Eshelby twist). NBED performed across smaller plates (which are sufficiently thin to remain transparent to the electron beam) shows that the diffraction patterns across the plates are identical to those in the adjacent nanowire sections, confirming that nanowires and plates have identical crystal orientation and seamless connection (Fig. 6(c)).

The presence of axial screw dislocations in a majority of VLS-grown GeS nanowires (and wire–plate heterostructures) synthesized on Si substrates and the absence of dislocations in nanostructures obtained on SnSe van der Waals substrates can help shed additional light on the dislocation formation, pointing to a mechanism where screw dislocations are introduced at the onset of VLS growth, *i.e.*, when the Au catalyst is still in contact with the substrate. As discussed above, in the case of growth on Si the actual growth “substrate” consists of spontaneously formed GeS plates covering small circular areas of the Si support (Fig. 1). Prior work showed that high-quality GeS flakes, (*e.g.*, grown on mica²⁷) frequently carry screw

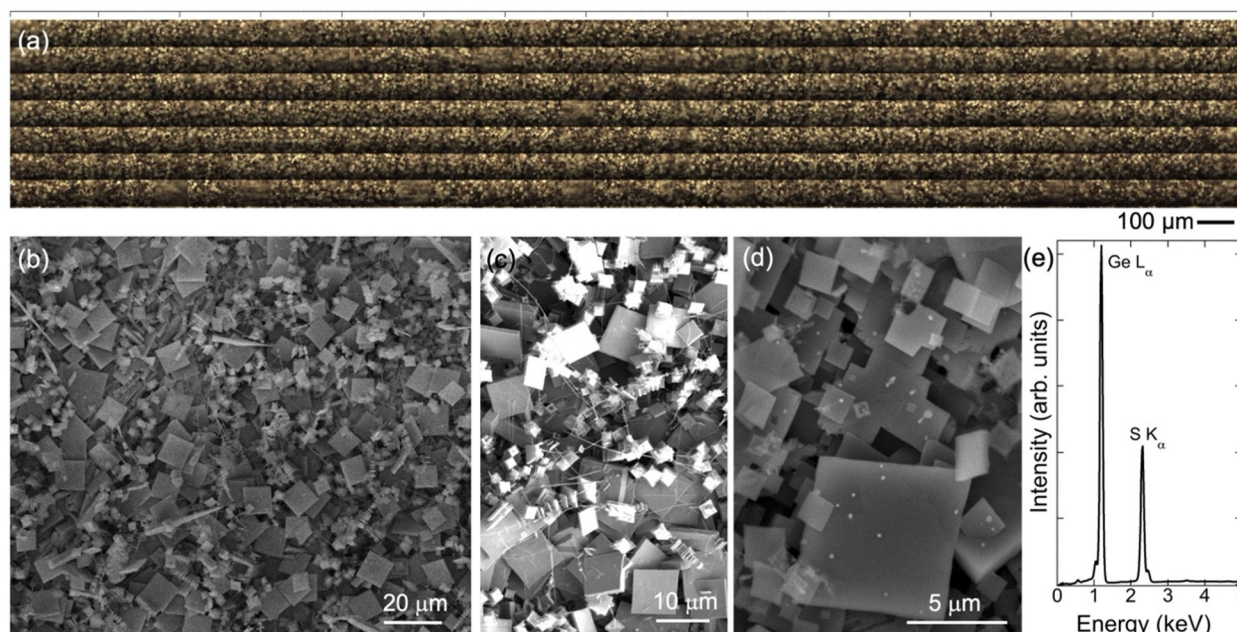


Fig. 4 Au-catalyzed GeS nanowire-plate heterostructures on SnSe/mica van der Waals substrates. (a) Large-area montage of top-view optical images of the dense forest of GeS mixed-dimensional heterostructures covering the entire Au/SnSe/mica surface. (b) Top-view SEM image of the heterostructures. (c) and (d) Higher magnification SEM images of the mixed-dimensional heterostructures. The hybrids frequently consist of plates with different sizes introduced at different positions along the GeS nanowires. (e) Characteristic EDS spectrum of the nanowire–plate heterostructures, yielding a composition of 51.5 at% Ge and 48.5 at% S.



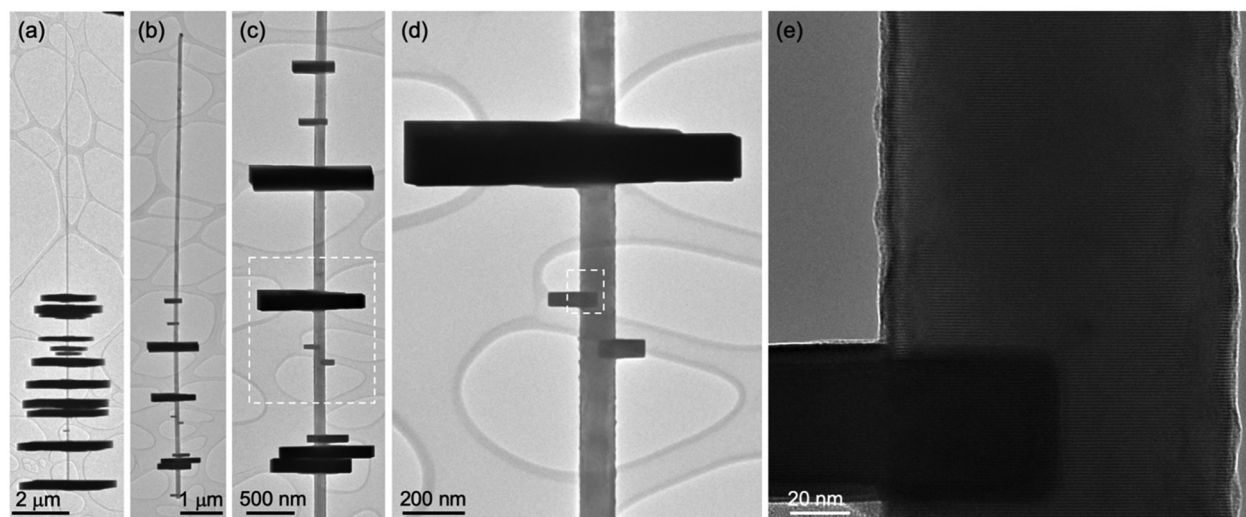


Fig. 5 Morphology of Au-catalyzed GeS mixed-dimensional heterostructures synthesized on Au/SnSe/mica. (a) and (b) TEM images of characteristic GeS nanowires (dispersed on lacey carbon support), grown over Au catalyst on SnSe/mica at a substrate temperature of 290 °C. The wires are decorated with multiple plates at different positions. (c) and (d) Higher magnification TEM images of part of the nanowire–plate heterostructure shown in (b). (e) High-resolution TEM image of the nanowire–plate heterostructure, obtained at the position marked with the dashed square in (d).

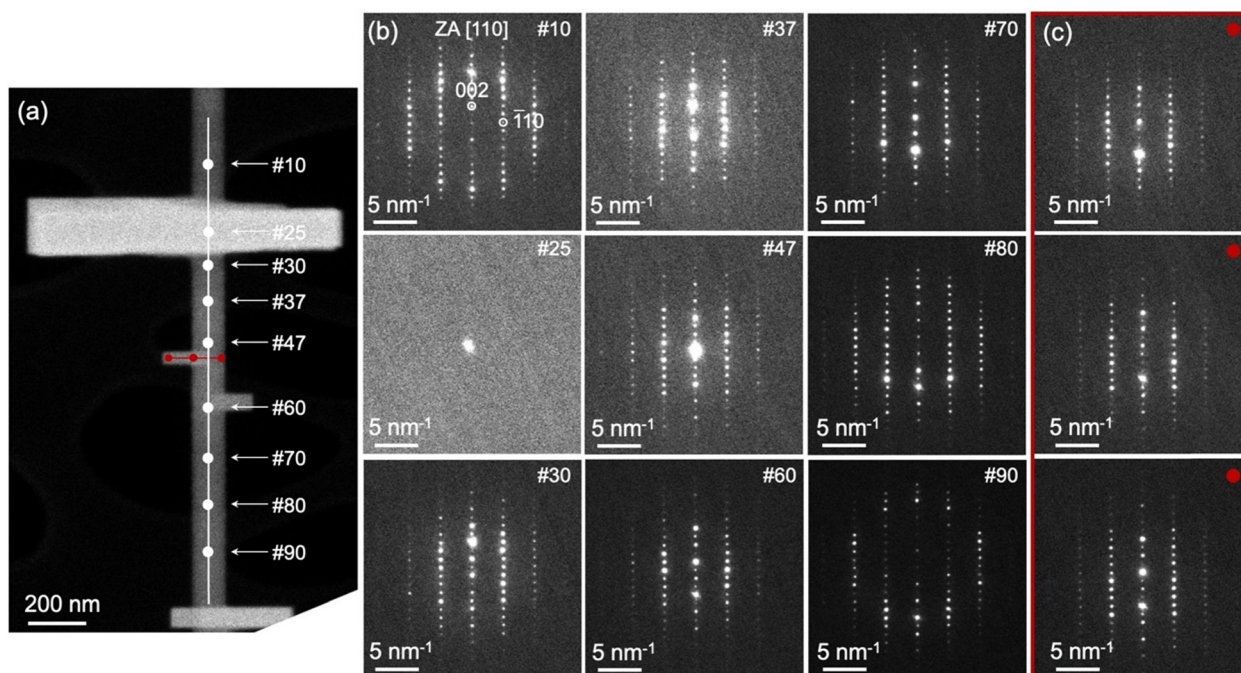


Fig. 6 Crystal structure of Au-catalyzed mixed-dimensional GeS heterostructures synthesized on SnSe/mica. (a) HAADF-STEM image of a segment of a GeS nanowire decorated with multiple GeS plates (see Fig. 5(c)). A sequence of 100 nanobeam electron diffraction patterns was obtained along the nanowire crossing both large and small plates (white line). A second sequence of 20 diffraction patterns was recorded along a small plate attached to the wire (red line). (b) Selected nanobeam electron diffraction patterns acquired at positions marked by dots and arrows along the white line in (a). All diffraction patterns are along the [110] zone axis (ZA) of the nanowire. There is no twist of the (a, b) crystal axes along the nanowire between the plates. Pattern #25 was taken at the position of a plate that is too thick to allow the diffracted electrons to emerge. (c) Selected nanobeam electron diffraction patterns acquired along the small plate (red line in (a)). The diffraction patterns show that the plate is viewed along the [110] ZA, *i.e.*, its crystal orientation is identical to the orientation of the nanowire.

dislocations. One can expect that the smaller GeS plates grown on Au/Si contain an even higher density of screw dislocations. In subsequent VLS growth, such defects serve as natural centers

for the formation of nanowires (or mixed dimensional heterostructures), where the screw dislocation in the substrate enables nucleation-less spiral growth of the VLS nanostructures. This is



consistent with the fact that electron microscopy invariably shows screw dislocations present all the way to the root end of the wires. VLS growth on SnSe/mica, on the other hand, occurs on a high-quality van der Waals substrate consisting of large, flat SnSe terraces that continuously cover the support. Prior results on SnSe growth on mica showed no propensity for screw dislocation formation²⁸ *i.e.*, the SnSe substrate can be expected to contain much fewer pre-existing dislocations that could be transferred into the VLS nanostructures, thus explaining their dislocation-free, single-crystalline structure.

The growth of mixed-dimensional GeS heterostructures on SnSe films requires the presence of a Au catalyst. In the absence of Au, the growth from GeS vapor resulted in GeS films and no growth of nanowires or heterostructures was observed. Bi was also deposited on the SnSe films and used as catalyst, analogous to VLS growth on Bi/Si(100) which showed complete coverage with GeS nanowires, albeit eliminating the mixed-dimensional heterostructures.¹⁹ GeS exposure of Bi covered SnSe van der Waals films did not result in the formation of nanowires but rather polycrystalline films, likely due to reaction of the Bi with the SnSe substrate. We also explored how the thickness of the Au film and the vapor pressure of the GeS precursor affect the growth of GeS nanostructures. Decreasing the GeS vapor pressure by lowering the temperature of the GeS precursor powder led to the formation of short single crystalline GeS nanowires. Growth at low GeS vapor pressure but increased Au coverage also leads to large GeS deposits at the base of the nanowires (Fig. S2).

Au catalyzed VLS growth on SnSe van der Waals support exhibits distinct differences to the growth on Si: (1) the entire

population consists of mixed dimensional heterostructures; (2) the heterostructures completely cover the substrates; and (3) the resulting GeS nanowires are single crystals without screw dislocations (and Eshelby twist). The absence of dislocations is expected to lead to homogeneous optoelectronic properties as these are strongly influenced by the presence of dislocations.

The optoelectronic properties of the mixed-dimensional heterostructures were probed by cathodoluminescence spectroscopy excited by the focused electron beam in STEM (STEM-CL). A focused ($\sim 1\text{--}2\text{ nm}$) electron beam was used as an excitation source for measuring light emission with nanometer spatial resolution. Fig. 7(a) and Fig. S3(a) show HAADF-STEM images of characteristic nanowire-plate heterostructures on which STEM-CL measurements were performed. Panchromatic CL maps of the two different heterostructures, shown in Fig. 7(b) and Fig. S3(b), display bright light emission across the heterostructures, with highest intensity of the emitted light originating from the vertically oriented plates. The emission along the nanowire segments between plates appears uniform (Fig. S3(b)). The mixed-dimensional GeS heterostructures, in which a nanowire supports a sequence of GeS plates, provide a unique geometry for achieving strong light emission. Indeed, as seen in Fig. 7(b) and Fig. S3(b), the plates represent a sequence of strong light emitters spaced along the nanowire backbone holding them together (which shows much lower emitted intensity due to the smaller thickness traversed by the exciting electron beam). In addition, the peak emission energies can be varied by changing the size of the plates, as we discuss below.

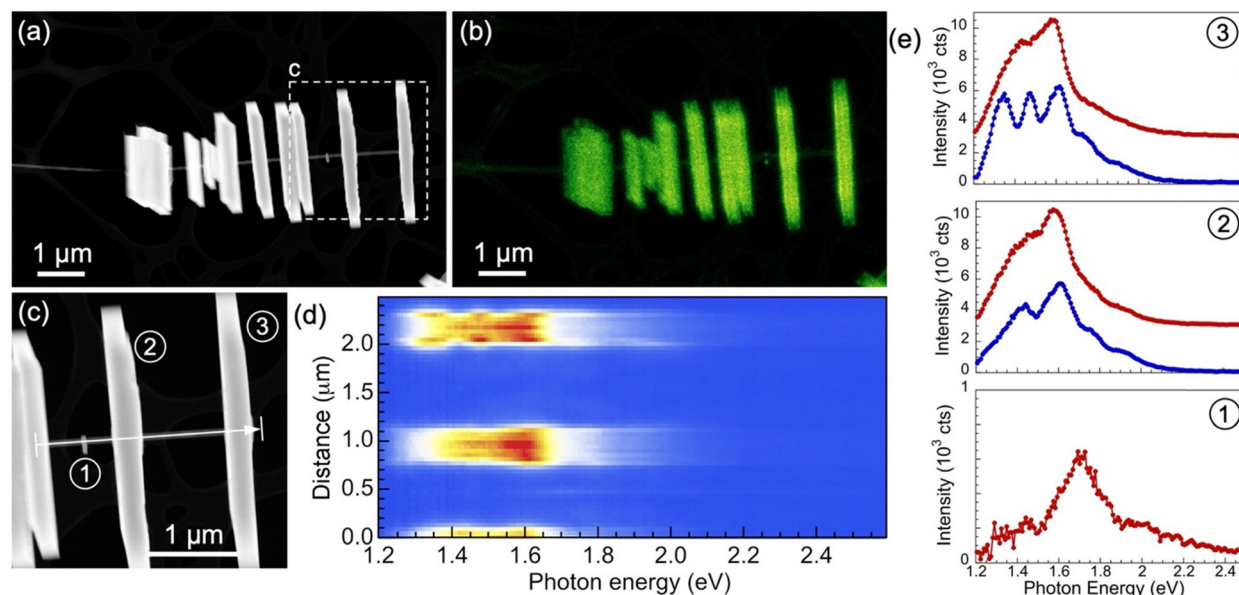


Fig. 7 STEM cathodoluminescence of mixed-dimensional GeS heterostructures. (a) STEM image of a portion of a mixed-dimensional GeS heterostructure. (b) Panchromatic STEM-CL image of the heterostructure in (a). (c) Higher magnification STEM image of part of the heterostructure (dashed box in (a)). (d) Hyperspectral CL linescan along the heterostructure, crossing three large and one small GeS plate (arrow in (c)). (e) CL spectra obtained at the position of three of the GeS plates in (c). Red spectra were obtained at the plate center, while blue spectra represent excitation near the surface of the plates.



Hyperspectral CL linescans, measured along the arrows in Fig. 7(c) and Fig. S3(a), were used to analyze the spectral composition of light emitted from the heterostructures (Fig. 7(d) and Fig. S3 (c)). The most intense peak in the CL emission from large plates (plates 2 and 3 in Fig. 7(c)) is centered at a photon energy $h\nu = 1.59$ eV. The spectral shape of the peak (red curves in Fig. 7(e)) shows the characteristic low-energy shoulder invariably present in GeS luminescence.^{29,30} This peak persists throughout the entire plate and stems from recombination across the fundamental bandgap of GeS.^{16,23,27} Near the surface of such large plates, additional discrete emission peaks with energies below the fundamental band gap are observed (blue curves in Fig. 7(e)). These sharp peaks are due to locally excited light emission in STEM-CL, which launches waveguide modes in the mesoscale GeS plates. The waveguide modes are internally reflected by the highly specular surface facets of the GeS plates, leading to constructive interference. Similar interference of edge-reflected waveguide modes is observed in the STEM-CL emission from horizontal plates, where it produces characteristic dispersive fringes.¹⁶ In the standing plates, the photonic modes give rise to intense, sharp peaks whose energies that can be controlled by the thickness of the plates. Plates 2 and 3 exhibit two and three of these sharp photonic peaks, respectively. In smaller plates (plate 1 in Fig. 7; plates marked by orange and yellow arrows in Fig. S3), light emission is confined to just one discrete energy correlated with photonic waveguide modes. The energy varies as a function of the thickness of the plates (from ~ 1.7 –2 eV) and is generally blue-shifted (Fig. S4) compared to the band-edge emission and the sub-bandgap interference peaks in large plates. The mixed-dimensional heterostructures therefore provide the ability to control the energy of emitted light *via* the size of the plates, in addition to conventional approaches to modify the bandgap (and hence the band-edge luminescence), such as alloying.¹⁸

3. Conclusions

In summary, we demonstrated the self-assembly of mixed-dimensional heterostructures combining 1D GeS nanowires and 2D GeS plates in a single-step vapor–liquid–solid growth process catalyzed by Au. To overcome the limited nucleation and growth in small, widely spaced areas on Au/Si(100) substrates, we explored growth on van der Waals substrates consisting of films in the form of coalesced, large (10–20 μm) SnSe flakes on mica. This approach was inspired by observations showing GeS nanowires and 1D–2D heterostructures on Si forming on spontaneously grown GeS plates in small areas of the substrate, which suggests that providing a pre-grown, quasi-continuous van der Waals surface could enable the controlled growth of GeS nanostructures across the entire substrate.

SEM and optical microscopy demonstrate that Au-catalyzed VLS growth on such SnSe van der Waals substrates indeed yields complete coverage with mixed-dimensional GeS heterostructures, consisting of GeS nanowires carrying GeS plates that

extend laterally from the nanowires. TEM and electron diffraction demonstrate that the nanowire and the plate segments have the same crystal structure and layer orientation, with the [001] (van der Waals) direction aligned along the axis of the vertical nanowire, templated by the basal plane of the underlying SnSe film. In contrast to GeS nanowires grown on Si(001), which invariably include screw dislocations and are thus chiral (with Eshelby twist), GeS nanowires formed on the SnSe films are layered single crystals that do not contain any dislocations. Analysis of the optoelectronic properties of individual 1D–2D GeS heterostructures using STEM-CL demonstrates that the mixed-dimensional heterostructures have a unique architecture combining a backbone in the form of GeS nanowires with relatively low emission with a sequence of attached GeS plates that are strong light emitters. The spectral content of the emission from large GeS plates is dominated by intense peak at 1.59 eV due to recombination across the band gap of GeS, along with sharp, intense peaks associated with interference of surface-reflected waveguide modes in the plates. Smaller plates show blue-shifted emission due to size-induced shifts of the energy of the selected GeS waveguide modes.¹⁸ Hence, the wavelength of the emitted light can be modified *via* the size of the plates, and the mixed dimensional heterostructures provide a pathway for achieving light emission with tunable energy and high intensity.

4. Materials and methods

4.1. Substrate preparation and characterization

Si(100) and SnSe/mica were used as growth substrates for the GeS nanowires and mixed-dimensional heterostructures. SnSe films were synthesized on mica in a pumped 2-inch quartz tube reactor with a single temperature-controlled zone. The SnSe (99.999%; ALB Materials) source powder was placed in a quartz boat in the center of the evaporation zone and heated to 570–580 °C. Freshly exfoliated mica substrates (Ted Pella) supported by a metal plate were placed with their leading edge 9 cm downstream from the source. During growth, an Ar (99.9999%; Matheson) carrier gas flow was maintained at 60 standard cubic centimeters per minute and a pressure of 20 mTorr. Growth was performed for periods of 30 and 45 minutes, after which the reactor was cooled naturally to room temperature. Prior to GeS growth, both Si(100) and SnSe/mica substrates were covered with Au films with nominal thickness of 2–10 nm by magnetron sputtering at room temperature. The Au films are known to dewet at the GeS growth temperature, thus providing an array of Au nanoparticles that served as catalysts for VLS growth of GeS nanostructures. Bi films were also deposited as catalyst for comparison.

van der Waals substrates consisting of SnSe films on mica were characterized using optical microscopy, SEM, and AFM. Polarized optical microscopy was performed in reflection geometry using an upright microscope (Olympus BX53) equipped with a fixed incident polarizer and adjustable reflected-light analyzer, a 100 \times objective, and a high-resolution (12.5 megapixel;



Olympus DP75) scientific camera. SEM was performed in a FEI Helios Nanolab 660 field-emission microscope at 5 keV primary beam energy. Energy-dispersive X-ray spectroscopy (EDS) was carried out SEM at 20 keV. AFM was performed in tapping mode using a Multimode microscope (Veeco), Nanoscope IV electronics, and a large-range (125 μm) scanner calibrated in (x, y, z) to within 2% using commercial calibration standards (Bruker).

4.2. GeS growth and characterization

GeS nanowires and mixed-dimensional heterostructures were synthesized in a separate pumped quartz tube reactor with two independently controlled temperature zones. GeS precursor powder (99.99%; ALB Materials) was placed in a quartz boat in the evaporation zone and heated to temperatures between 400–450 °C (corresponding to vapor pressures P_{GeS} between 0.0556–0.288 Torr). GeS growth on Si(100) covered with 2 nm thick Au films was carried out at a growth temperature of 300 °C.²⁶ GeS growth on SnSe/mica substrates with and without Au was carried out at temperatures between 280–300 °C. During all growths, an Ar (99.9999%, Matheson) carrier gas flow was maintained at 60 standard cubic centimeters per minute (sccm) at a pressure of 20 mTorr. The growth was typically performed for 5 minutes, resulting in the formation of forests of nanowires with lengths of several tens of micrometers. Nanowire forests on the native growth substrates were imaged using optical microscopy and SEM. Structure and morphology of individual nanowires were investigated by transmission electron microscopy (TEM) in an FEI Talos F200X microscope. For the TEM experiments thousands of nanowires were spread on lacey carbon supports. Cathodoluminescence measurements were performed in HAADF-STEM at room temperature using a Gatan Vulcan CL holder and an incident electron beam current of 420 pA on samples prepared by dry transfer from the growth substrate to lacey carbon grids. Panchromatic CL maps (integrating from $400\text{ nm} \leq \lambda \leq 1000\text{ nm}$) were acquired with 512×512 pixels at 2 ms per pixel. Hyperspectral CL linescans were obtained by positioning the exciting beam at equidistant points along a selected trajectory and acquiring full spectra at each point by dispersing the emitted light in a spectrometer equipped with a cooled Si CCD detector (integration time: 10 s per spectrum).

Conflicts of interest

The authors declare no conflicts of interest.

Data availability

The data supporting this article has been included as part of the supplementary information (SI). Supplementary information: figures: TEM images and electron diffraction patterns of Au-catalyzed GeS nanowires and mixed-dimensional GeS heterostructures synthesized on SnSe/mica and STEM-CL of mixed-dimensional GeS heterostructures; peak photon energies

as a function of the plates thicknesses. Raw data. (PDF). See DOI: <https://doi.org/10.1039/d5ma00694e>.

Acknowledgements

This work was supported by the National Science Foundation, Division of Materials Research, Solid State and Materials Chemistry Program under grant no. DMR-2315397. SEM and EDS investigations were performed in the Nebraska Nanoscale Facility: National Nanotechnology Coordinated Infrastructure and the Nebraska Center for Materials and Nanoscience, which are supported by the National Science Foundation under Award ECCS: 2025298, and the Nebraska Research Initiative. The authors thank J. French, P. Ghimire, H. Saraswat and Sh. Shamim for technical support.

References

- 1 A. Castellanos-Gomez, X. Duan, Z. Fei, H. R. Gutierrez, Y. Huang, X. Huang, J. Quereda, Q. Qian, E. Sutter and P. Sutter, van der Waals heterostructures, *Nat. Rev. Methods Primers*, 2022, **2**, 58, DOI: [10.1038/s43586-022-00139-1](https://doi.org/10.1038/s43586-022-00139-1).
- 2 K. Lee, X. Duan, M. C. Hersam and J. Kim, Fundamentals and applications of mixed-dimensional heterostructures, *APL Mater.*, 2022, **10**, 060402, DOI: [10.1063/5.0097804](https://doi.org/10.1063/5.0097804).
- 3 B. Xu, P. He, H. Liu, P. Wang, G. Zhou and X. Wang, A 1D/2D Helical CdS/ZnIn₂S₄ Nano-Heterostructure, *Angew. Chem., Int. Ed.*, 2014, **53**, 2339–2343, DOI: [10.1002/anie.201310513](https://doi.org/10.1002/anie.201310513).
- 4 Y. Fu, Y. Wang, Y. Wu, C. Feng, H. Zhang and Y. Wang, Epitaxial growth of cactus-like heterojunction with perfect interface for efficient photoelectrochemical water splitting, *Chem. Eng. J.*, 2023, **452**, 139406, DOI: [10.1016/j.cej.2022.139406](https://doi.org/10.1016/j.cej.2022.139406).
- 5 X. Li, Z. Jiang, F. Ge, C.-L. Tao, W. Gu, D. Xu, F. Chen, Z. Xie, F. Cheng and X.-J. Wu, Generalized Colloidal Approach for Preparing Epitaxial 1D/2D Heterostructures, *Chem. Mater.*, 2022, **34**, 4577–4586, DOI: [10.1021/acs.chemmater.2c00424](https://doi.org/10.1021/acs.chemmater.2c00424).
- 6 Z. Ge, C. Wang and L. Qi, Controllable synthesis of hierarchical Au/PdAg heterostructures consisting of nanosheets on nanorods with plasmon-enhanced electrocatalytic properties, *Inorg. Chem. Front.*, 2020, **7**, 4077–4085, DOI: [10.1039/D0QI00945H](https://doi.org/10.1039/D0QI00945H).
- 7 G. Liu, C. Kolodziej, R. Jin, S. Qi, Y. Lou, J. Chen, D. Jiang, Y. Zhao and C. Burda, MoS₂-Stratified CdS–Cu_{2–x}S Core–Shell Nanorods for Highly Efficient Photocatalytic Hydrogen Production, *ACS Nano*, 2020, **14**, 5468–5479, DOI: [10.1021/acsnano.9b09470](https://doi.org/10.1021/acsnano.9b09470).
- 8 X. Yang, R. Wu, B. Zheng, Z. Luo, W. You, H. Liu, L. Li, Y. Zhang, Q. Tan, D. Liang, Y. Chen, J. Qu, X. Yi, X. Wang, J. Zhou, H. Duan, S. Wang, S. Chen, A. Pan and A. Waveguide-Integrated Two-Dimensional Light-Emitting Diode Based, on p-Type WSe₂/n-Type CdS Nanoribbon Heterojunction, *ACS Nano*, 2022, **16**, 4371–4378, DOI: [10.1021/acsnano.1c10607](https://doi.org/10.1021/acsnano.1c10607).



- 9 H. Kong, H. Yao, Y. Li, Q. Wang, X. Qiu, J. Yan, J. Zhu and Y. Wang, Mixed-Dimensional van der Waals Heterostructures for Boosting Electricity Generation, *ACS Nano*, 2023, **17**, 18456–18469, DOI: [10.1021/acsnano.3c06080](https://doi.org/10.1021/acsnano.3c06080).
- 10 Y. T. Lee, P. J. Jeon, J. H. Han, J. Ahn, H. S. Lee, J. Y. Lim, W. K. Choi, J. D. Song, M.-C. Park, S. Im and D. K. Hwang, Mixed-Dimensional 1D ZnO–2D WSe₂ van der Waals Heterojunction Device for Photosensors, *Adv. Funct. Mater.*, 2017, **27**, 1703822, DOI: [10.1002/adfm.201703822](https://doi.org/10.1002/adfm.201703822).
- 11 J. Chen, X.-J. Wu, Y. Gong, Y. Zhu, Z. Yang, B. Li, Q. Lu, Y. Yu, S. Han, Z. Zhang, Y. Zong, Y. Han, L. Gu and H. Zhang, Edge Epitaxy of Two-Dimensional MoSe₂ and MoS₂ Nanosheets on One-Dimensional Nanowires, *J. Am. Chem. Soc.*, 2017, **139**, 8653–8660, DOI: [10.1021/jacs.7b03752](https://doi.org/10.1021/jacs.7b03752).
- 12 H. Song, S. Ji, S. G. Kang and N. Shin, Contact Geometry-Dependent Excitonic Emission in Mixed-Dimensional van der Waals Heterostructures, *ACS Nano*, 2024, **18**, 19179–19189, DOI: [10.1021/acsnano.4c04770](https://doi.org/10.1021/acsnano.4c04770).
- 13 K. Jiang, Q. You, Y. Zheng, F. Fang, Z. Xie, H. Li, Y. Wan, C. Han and Y. Shi, Oriented Epitaxial Growth of Mixed-Dimensional van der Waals Heterostructures with One-Dimensional (1D) Bi₂S₃ Nanowires and Two-Dimensional (2D) WS₂ Monolayers for Performance-Enhanced Photodetectors, *Nano Lett.*, 2024, **24**, 14437–14444, DOI: [10.1021/acs.nanolett.4c04455](https://doi.org/10.1021/acs.nanolett.4c04455).
- 14 Q. Wu, Z. Fang, Y. Zhu, H. Song, Y. Liu, X. Su, D. Pan, Y. Gao, P. Wang, S. Yan, Z. Fei, J. Yao and Y. Shi, Controllable Edge Epitaxy of Helical GeSe/GeS Heterostructures, *Nano Lett.*, 2022, **22**, 5086–5093, DOI: [10.1021/acs.nanolett.2c00395](https://doi.org/10.1021/acs.nanolett.2c00395).
- 15 G. Lu, Y. Wei, X. Li, G. Zhang, G. Wang, L. Liang, Q. Li, S. Fan and Y. Zhang, Reconfigurable Tunneling Transistors Heterostructured by an Individual Carbon Nanotube and MoS₂, *Nano Lett.*, 2021, **21**, 6843–6850, DOI: [10.1021/acs.nanolett.1c01833](https://doi.org/10.1021/acs.nanolett.1c01833).
- 16 P. Sutter, C. Argyropoulos and E. Sutter, Germanium Sulfide Nano-Optics Probed by STEM-Cathodoluminescence Spectroscopy, *Nano Lett.*, 2018, **18**, 4576–4583, DOI: [10.1021/acs.nanolett.8b01840](https://doi.org/10.1021/acs.nanolett.8b01840).
- 17 C. Li, Y. Yu, M. Chi and L. Cao, Epitaxial Nanosheet–Nanowire Heterostructures, *Nano Lett.*, 2013, **13**, 948–953, DOI: [10.1021/nl303876a](https://doi.org/10.1021/nl303876a).
- 18 E. Sutter and P. Sutter, Self-Assembly of Mixed-Dimensional GeS₁–xSex (1D Nanowire)–(2D Plate) van der Waals Heterostructures, *Small*, 2023, **19**, 2302592, DOI: [10.1002/smll.202302592](https://doi.org/10.1002/smll.202302592).
- 19 E. Sutter and P. Sutter, Ultrathin Twisted Germanium Sulfide van der Waals Nanowires by Bismuth Catalyzed Vapor–Liquid–Solid Growth, *Small*, 2021, **17**, 2104784, DOI: [10.1002/smll.202104784](https://doi.org/10.1002/smll.202104784).
- 20 H. Shim, N. Shin and V. L. S. Homoepitaxy, of Lead Iodide Nanowires for Hybrid Perovskite Conversion, *The, J. Phys. Chem. Lett.*, 2019, **10**, 6741–6749, DOI: [10.1021/acs.jpclett.9b02543](https://doi.org/10.1021/acs.jpclett.9b02543).
- 21 E. Sutter, B. Ozturk and P. Sutter, Selective growth of Ge nanowires by low-temperature thermal evaporation, *Nanotechnology*, 2008, **19**, 435607, DOI: [10.1088/0957-4484/19/43/435607](https://doi.org/10.1088/0957-4484/19/43/435607).
- 22 E. Sutter and P. Sutter, 1D Wires of 2D Layered Materials: Germanium Sulfide Nanowires as Efficient Light Emitters, *ACS Appl. Nano Mater.*, 2018, **1**, 1042–1049, DOI: [10.1021/acsanm.7b00053](https://doi.org/10.1021/acsanm.7b00053).
- 23 P. Sutter, J.-C. Idrobo and E. Sutter, van der Waals Nanowires with Continuously Variable Interlayer Twist and Twist Homojunctions, *Adv. Funct. Mater.*, 2021, **31**, 2006412, DOI: [10.1002/adfm.202006412](https://doi.org/10.1002/adfm.202006412).
- 24 R. S. Wagner and W. C. Ellis, Vapor–liquid–solid mechanism of single crystal growth, *Appl. Phys. Lett.*, 1964, **4**, 89–90, DOI: [10.1063/1.1753975](https://doi.org/10.1063/1.1753975).
- 25 P. Sutter, S. Wimer and E. Sutter, Chiral twisted van der Waals nanowires, *Nature*, 2019, **570**, 354–357, DOI: [10.1038/s41586-019-1147-x](https://doi.org/10.1038/s41586-019-1147-x).
- 26 P. Sutter and E. Sutter, Tunable 1D van der Waals Nanostructures by Vapor–Liquid–Solid Growth, *Acc. Chem. Res.*, 2023, **56**, 3235–3245, DOI: [10.1021/acs.accounts.3c00502](https://doi.org/10.1021/acs.accounts.3c00502).
- 27 E. Sutter, B. Zhang, M. Sun and P. Sutter, Few-Layer to Multilayer Germanium(II) Sulfide: Synthesis, Structure, Stability, and Optoelectronics, *ACS Nano*, 2019, **13**, 9352–9362, DOI: [10.1021/acsnano.9b03986](https://doi.org/10.1021/acsnano.9b03986).
- 28 E. Sutter, P. Ghimire and P. Sutter, Macroscopic Monochalcogenide van der Waals Ferroics: Growth, Domain Structures, and Curie Temperature, *J. Am. Chem. Soc.*, 2024, **146**, 31961–31968, DOI: [10.1021/jacs.4c11558](https://doi.org/10.1021/jacs.4c11558).
- 29 P. Sutter, L. Khosravi-Khorashad, C. V. Ciobanu and E. Sutter, Chirality and dislocation effects in single nanostructures probed by whispering gallery modes, *Mater. Horiz.*, 2023, **10**(9), 3830, DOI: [10.1039/D3MH00693J](https://doi.org/10.1039/D3MH00693J).
- 30 E. Sutter, J. S. French, H.-P. Komsa and P. Sutter, 1D Germanium Sulfide van der Waals Bicrystals by Vapor–Liquid–Solid Growth, *ACS Nano*, 2022, **16**, 3735–3743, DOI: [10.1021/acsnano.1c07349](https://doi.org/10.1021/acsnano.1c07349).

